IIETA International Information and Engineering Technology Association
Advancing the World of Information and Engineering

Journal of New Materials for Electrochemical Systems
Vol.25, No.2, April 2022, pp. 98-102
Journal homepage: http://iieta.org/journals/jnmes

Improving high-temperature cycle stability and rate performance of $LiNi_{0.82}Co_{0.11}Mn_{0.07}O_2$ cathode materials using hydrogen peroxide solution washing System

Seon-Jin Lee, Hyun-Ju Jang and Jong-Tae Son*

Department of Nano-Polymer Science & Engineering, Korea National University of Transportation, Chungju, Chungbuk 27469, Republic of Korea.

Corresponding author email: jt1234@ut.ac.kr

https://doi.org/10.14447/jnmes.v25i2.a02

Received: July 21-2021
Accepted: May 5-2022

Keywords:
Ni-rich materials, Li residuals, H_2O_2, Washing process

ABSTRACT

In this study, for the removal of residual lithium (Li_2CO_3, LiOH) from a nickel-rich cathode material surface, $LiNi_{0.82}Co_{0.11}Mn_{0.07}O_2$ cathode materials were washed with an aqueous solution of hydrogen peroxide (H_2O_2). H_2O_2 (pH 6.04), a weak acid, can easily decompose Li_2CO_3 and LiOH as an oxidizing agent. On titration of residual lithium, the amounts of LiOH and Li_2CO_3 are 390 and 605 ppm, 25- and 47-times lower, after H_2O_2 washing compared to 10,296 and 28,440 ppm, respectively, in case of cathode materials before washing. On DSC thermal analysis, the peak temperature and calorific value of the cathode material washed with H_2O_2 were 245.5 °C and 602.0 J/g, respectively, whereas the bare case was 208.6 °C and 1,071 J/g, respectively. Therefore, H_2O_2-washed $LiNi_{0.82}Co_{0.11}Mn_{0.07}O_2$ cathode materials had higher capacity heat retention after 100 cycles at 55 °C (85.6% at 0.5C) than the bare $LiNi_{0.82}Co_{0.11}Mn_{0.07}O_2$ cathode materials (78.6% at 0.5C).

1. INTRODUCTION

The Lithium-ion batteries (LIBs) have gained increased research attention as the most advanced energy storage devices being widely used in portable electronics and electric vehicles.[1,2] These applications require further energy density promotion and cost reduction in LIBs, which are mainly determined by the cathode materials.[3] Therefore, materials with Ni contents greater than 80% are the most favorable cathode materials for EV applications owing to their high capacity (~220 mAh/g) and low manufacturing costs compared to conventional $LiCoO_2$ materials.[4-6]

However, major drawbacks of structural degradation, gas evolution, cation mixing, and the presence of a large amount of Li_2CO_3 or LiOH on the surface must be overcome for successful commercialization.[7-11] The removal of Li residuals from Ni-rich materials is a key problem that needs to be solved because the presence of Li residuals poses the potential risk of gas evolution on the surface.[12,13]

To address these problems in the industrial field, a water-washing process is introduced to reduce Li residues. However, Tasaki et al.[14] reported that Li_2CO_3 in water (1.3 g per 100 mL) has lower solubility than LiOH (12.8 g per 100 mL) at 25 ℃, although it possesses excellent electrochemical inertness, the exposed Li_2CO_3 particles easily react with $LiPF_6$ based electrolyte and $LiPF_6$ powder to generate LiF, CO_2, and POF_3.[15]. Therefore, it is important to simultaneously remove LiOH and Li_2CO_3 to enable the commercialization of nickel-rich cathode materials. Park et al.[16] succeeded in reducing the amount of Li_2CO_3 to 2,890 ppm and LiOH to 5,800 ppm by using a nitric acid aqueous solution solvent evaporation process. Park et al.[17] selected a water/active substance (1:1 ratio) and a drying temperature of 120 °C as the optimal washing condition to reduce the total residual lithium content by 1/3 while minimizing cell performance degradation. However, until now, although research results for removing residual lithium have been effective at 25 °C, concerns about thermal stability at high temperatures (>50 °C) remain.

To solve this problem, in this study, $LiNi_{0.82}Co_{0.11}Mn_{0.07}O_2$ cathode materials were washed with an aqueous solution of H_2O_2. H_2O_2 (pH 6.04), a weak acid, can easily decompose Li_2CO_3 and LiOH as an oxidizing agent. It effectively removes LiOH and reacts with Li_2CO_3, given by reactions (1) and (2) [18] for removal of residual lithium.

$$Li_2CO_3 + H_2O_2 \rightarrow 2LiOH + CO_2 + 1/2O_2 \quad (1)$$

$$LiOH\,(aq) \rightarrow H^+\,(aq) + OH^-\,(aq) \quad (2)$$

To the best of our knowledge, no study has reported a H_2O_2 aqueous solution washing process for the removal of residual lithium from $LiNi_{0.82}Co_{0.11}Mn_{0.07}O_2$ cathode materials.

2. EXPERIMENT

2.1 Preparation of $LiNi_{0.82}Co_{0.11}Mn_{0.07}O_2$

A commercially available $LiNi_{0.82}Co_{0.11}Mn_{0.07}(OH)_2$ precursor (ECOPRO Corp., Korea) was ground with a stoichiometric amount of $LiOH{\cdot}H_2O$. Subsequently, the pristine NCM material was obtained after the ground material was calcined at 750 °C for 15 h in O_2.

2.2 Washing process of $LiNi_{0.82}Co_{0.11}Mn_{0.07}O_2$

For the H_2O_2 washing process, 1 g of $LiNi_{0.82}Co_{0.11}Mn_{0.07}O_2$ powder (NCM) was dissolved in 100 g of solvents, one of

which was DI water and the other was a mixture of DI water and H_2O_2 (0.01 M). The solution of NCM powder and solvent was stirred for 60 min and dried at 120 °C until the solvent completely evaporated. H_2O_2-washed NCM and water-washed NCM were prepared after the solvent-dried NCM powders were heated at 750 °C for 10 h under O_2 flow.

2.3. Material characterization

X-ray diffraction patterns for the cathodes were obtained using a Siemens D-5000 diffractometer in the 2θ range of 10° to 80° with Cu Kα radiation (λ = 1.5406 Å). The obtained powder morphology was observed using scanning electron microscopy (SEM, JSM-7610F, JEOL). The surface area and surface morphology of the obtained powders were observed using an atomic force microscope (N3-AM, Bruker).

2.4. Electrochemical characterization

To prepare the positive electrode, 0.8 g $LiNi_{0.82}Co_{0.11}Mn_{0.07}O_2$ powder 0.1 g Super-P (Aldrich), N-methyl-2-pyrrolidone (NMP), and 0.1 g PVDF (Kureha KF100) binder were mixed. Subsequently, the slurry was applied on aluminum foil using a doctor blade to form a film (thickness, 25 μm). The electrode was dried at 120 °C for 4 h in a vacuum-drying oven. The CR2032-type coin cell was combined in a glovebox using a $LiNi_{0.82}Co_{0.11}Mn_{0.07}O_2$ cathode electrode, lithium metal (as anode), porous polypropylene, and a 1M $LiPF_6$ solution with a 7:3 volume ratio of dimethyl carbonate (DMC)/ethylene carbonate (EC). The electrodes were charged and discharged galvano-statically from 3.0 to 4.3 V versus Li/Li^+ at a continuous current of 85 mAg^{-1} (0.5 C). Cycle performances at 55 ° C were evaluated at 85 mAg^{-1} (0.5 C).

3. RESULTS AND DISCUSSION

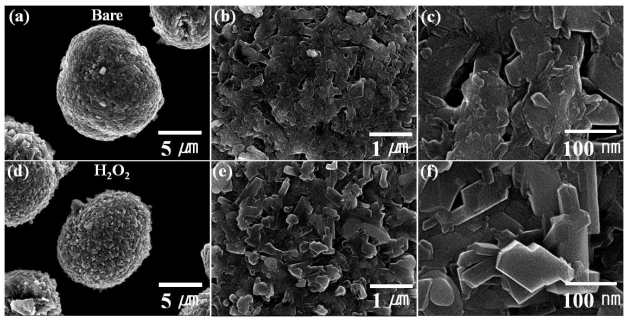

Figure 1. SEM images of the (a-c) bare and (d-f) H_2O_2-washed cathode materials.

Figure 1 shows SEM images of the bare and H2O2-washed cathode materials. Notably, the particles adopt a spherical morphology in the secondary particles and the estimated particle diameter is approximately 13–15 μm, as shown in Figure 1 (a, d). Figure 1 (b, e) shows that the primary particle shapes were not clearly identified. Figure 1(c) shows that the primary particles are rounded with many large protrusions on the surface; however, Figure 1(f) shows they are right-angled with fine-sized protrusions.

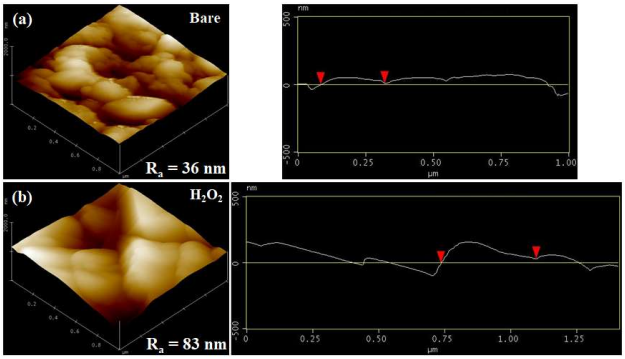

Figure 2. AFM images of the (a) bare and (b) H_2O_2-washed cathode materials.

Figure 2(a, b) shows AFM images of the bare and H_2O_2-washed cathode materials. Compared with the bare sample, the average roughness (R_a) after H_2O_2-washing increased from 36 to 83 nm. This increased surface area is owing to the removal of residual lithium from the cathode materials surface.

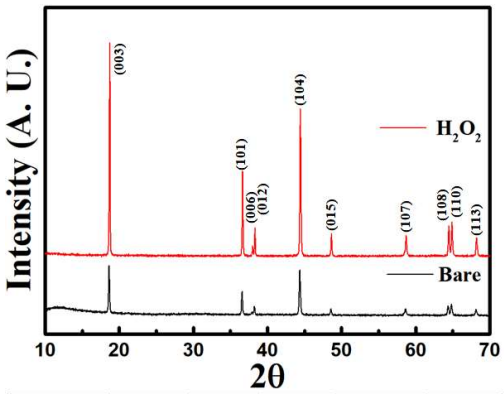

	a (Å)	c (Å)	V	(003)/(104)	R-factor
Bare	2.871	14.197 (± 0.001)	101.329	1.15	0.47
H_2O_2	2.868 (± 0.001)	14.208 (± 0.001)	101.316	1.28	0.44

Figure 3. XRD analysis of the bare and H_2O_2-washed cathode materials.

Figure 3 shows XRD patterns of the bare and H_2O_2-washed cathode materials. All peaks correspond to the layered α-$NaFeO_2$ structure of the space group R-3m without any impurities. The H_2O_2-washed cathode had a larger c-axis lattice parameter than the bare cathode. The lithium in the structure is presumed to be desorbed during the H_2O_2 washing process, thereby increasing the repulsive force between oxygen in the cathode structure. Owing to the reduction of lithium in the structure, the cation-mixing phenomenon in the structure decreased and the peak value of $I_{(003)}/I_{(104)}$ increased after H_2O_2 washing. However, after the R-factor analysis, which determines the degree of crystallinity of hexagonal, the structure became well-ordered after washing with H_2O_2 was confirmed.

The Li residuals amount is closely related to the cation-mixing behavior because the unoccupied Li ions in the Li layer can be transformed into Li residuals. The amounts of LiOH and Li_2CO_3 are calculated and obtained using equations (3) and (4) [19,20]:

$$LiOH + HCl \rightarrow LiCl + H_2O \quad (3)$$
$$Li_2CO_3 + 2HCl \rightarrow 2LiCl + H_2O + CO_2 \quad (4)$$

Li residuals amounts in the pristine and coated samples are listed in Table 1. The LiOH amount is 390 ppm, which is 25-times lower after H_2O_2 washing compared to 10,296 ppm of the cathode materials before washing, and Li_2CO_3 is 605 ppm, which is 47-times lower after washing compared to 28,440 ppm of the cathode materials before washing. It is noted that the total amount of Li residuals in the reheated NCMs are subjected to the H_2O_2 washing process.

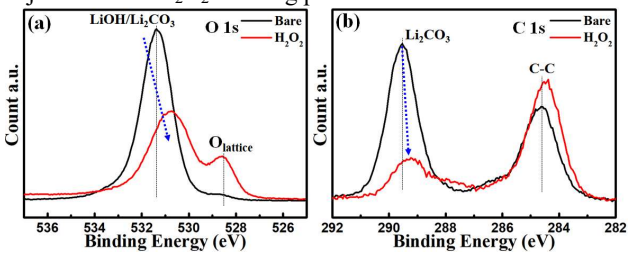

Figure 4. XPS spectra of (a) O 1s and (b) C 1s of the bare and H_2O_2-washed cathode materials.

The amounts of $LiOH/Li_2CO_3$ used to indicate residual lithium and oxygen from the bare and H_2O_2-washed NCM lattices (O lattice) that were present throughout the active material were investigated by X-ray photoelectron spectroscopy (XPS) profiles; the results are shown in Figure 4(a). The lower binding energy peak of 528.8 eV was assigned to the O lattice and higher binding energy peak of 531 eV was assigned to residual lithium species, such as Li_2CO_3 and LiOH. After H_2O_2 washing, the peak amount around 531 eV decreased owing to the reduced residual lithium. Additionally, it was confirmed that the peak amount indicating the amount of O lattice around 528.8 eV increased as the surface residual lithium layer thickness decreased. The C 1s spectra collected on the high-Ni materials contain species from Li_2CO_3 (289.8 eV) and adventitious carbon (centered near 284.8 eV and 286.0 eV), as shown in Figure 4(b).[21]

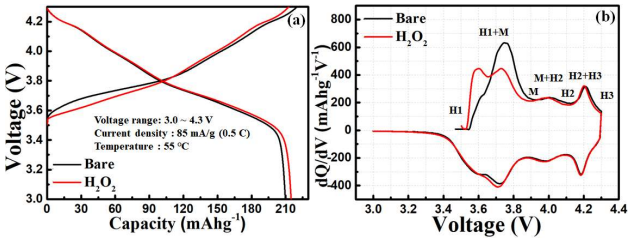

Figure 5. (a) Initial charge–discharge and (b) differential capacity (dQ/dV) curves of bare and H_2O_2-washed cathode materials.

The charge–discharge curves of the bare and H_2O_2-washed cathode materials were evaluated at a current density of 17 mA/g at 55 °C in the voltage range of 3.0–4.3 V, as shown in Figure 5(a). The discharge capacity of bare and H_2O_2-washed cathode materials is 209.7 and 214.8 mAh/g, respectively. The discharge capacity of the H_2O_2-washed material was higher than that of the bare material. The increased discharge capacity was due to the increased surface area after H_2O_2 washing. To confirm reduced lithium residual effect during cycling, the dQ/dV profiles of both the cathode materials were obtained by differentiating the charge–discharge curves, as shown **in** Figure 5(b). As the impediment to lithium-ion migration was reduced owing to the removal of the surface residual lithium, the overvoltage of the initial oxidation peak during charging decreased after H_2O_2 washing. Therefore, the discharge capacity has increased and the rate performances are expected to improve.

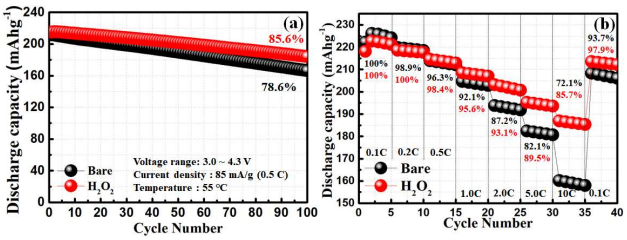

Figure 6. (a) Cycle performance and (b) rate capability of bare and H_2O_2-washed cathode materials.

Figure 6(a) shows the cycling performance of the bare and H_2O_2-washed cathode materials at 55 °C. Although the cell based on Bare retained only 78.6 % of its initial capacity after 100 cycles, the H_2O_2-washed cathode materials showed a capacity retention of 85.6 %. This result suggests that the side reaction between the residual lithium and the electrolyte after washing with H_2O_2 was suppressed.

Rate capability is an important electrochemical characteristic of Li-ion batteries for electric and hybrid electric vehicles. Figure 6(b) shows the rate capability of the bare and H_2O_2-washed cathode materials at 55 °C. The H_2O_2-washed cathode materials exhibited higher capacity than the bare and Al-doped electrodes (0.5 C), which further demonstrates the enhanced rate performance. The discharge capacity of the bare is presumed high before 0.5 C because the content of lithium is higher than the result of H_2O_2 washing. After 0.5 C, the rate performances were enhanced owing to the reduced residual lithium effect after washing with H_2O_2. The side reaction products have more negative effect of the cell performances. The benefit effect of the washing at high rate than at low rate. After 35 cycles, the cells maintained 93.7% its initial capacity (without washing) and 97.9% its initial capacity (after washing) at 0.1C. The improvement in rate stability could explained by the washing process which removed residual lithium in cathode material.

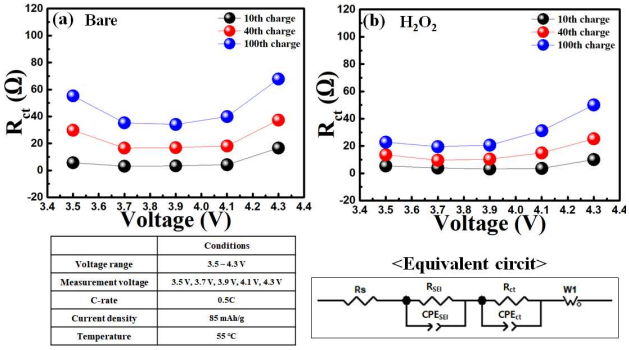

Figure 7. Difference in charge transfer resistance as a function of voltage of (a) bare and (b) H_2O_2-washed cathode electrodes.

Figure 7(a) and (b) show the AC impedance spectrum and the difference in charge transfer resistance as a function of voltage of bare and H_2O_2-washed cathode materials. The electrode data show R_{SEI} and R_{ct}, indicating solid electrolyte interphase resistance (R_{SEI}) and charge transfer resistance (R_{ct}). The semicircle at low frequencies reflects the R_{ct} and interfacial capacitance between the electrodes and electrolyte, and the semicircle at high frequencies reflects the charge transfer resistance.[21,22] We can obtain information on the cathode surface during cycling from the second semicircle, which reflects R_{ct}. It is clear from Figure 7(b) that a pronounced difference appears at the R_{ct} of 4.3V. H_2O_2-washed cathode materials exhibit low R_{ct} in all voltage ranges compared to bare cathode materials, as shown in Figure 7.

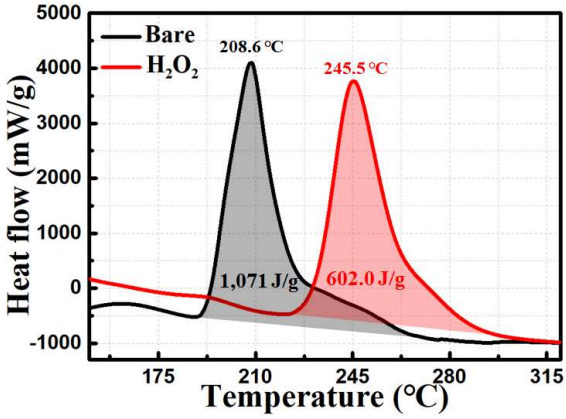

Figure 8. DSC traces of the bare and H_2O_2-washed cathode materials charged to 4.3 V.

Figure 8 shows the DSC profiles of the bare and H_2O_2-washed cathode materials charged to 4.3 V in the presence of a 1 M $LiPF_6$/EC:DEC electrolyte. For the bare material, the onset temperature of the exothermic reaction peak was 208.6 °C. In contrast, the H_2O_2-washed cathode materials showed higher onset temperatures and reduced heat generation compared to the bare cathode material. The high thermal stability of the H_2O_2-washed cathode materials suggests that the reduced residual lithium effectively suppresses the exothermic reaction.

4. CONCLUSIONS

$LiNi_{0.82}Co_{0.11}Mn_{0.07}O_2$ cathode materials were washed with a H_2O_2 aqueous solution. The residual amount of LiOH and Li_2CO_3 were 390 and 605 ppm, which is 25- and 47-times lower after H_2O_2 washing, compared to 10,296 and 28440 ppm, respectively, in the cathode materials before washing. R_{ct} decreased in all voltage ranges during charging owing to the reduced residual lithium after H_2O_2 washing. The discharge capacity of bare and H_2O_2-washed cathode materials was 209.7 and 214.8 mAh/g, respectively. The H_2O_2-washed $LiNi_{0.82}Co_{0.11}Mn_{0.07}O_2$ cathode materials exhibited higher capacity retention after 100 cycles at 55 °C (85.6% at 0.5C) than the bare $LiNi_{0.82}Co_{0.11}Mn_{0.07}O_2$ cathode materials (72% at 0.5C). DSC thermal analysis results showed that the peak temperature and calorific value of the cathode material washed with H_2O_2 were 245.5 °C and 602.0 J/g, respectively, whereas in case of the bare material, these were 208.6 °C and 1071 J/g, respectively. The high thermal stability of the H_2O_2-washed cathode materials suggests that the reduced residual lithium effectively suppresses exothermic reactions.

ACKNOWLEDGMENT

This study was supported by a grant from the Ministry of SMEs and Startups, Republic of Korea (S3045542) and the National Research Foundation of Korea (NRF) funded by the Korean Government (MSIT, No. This study was supported by the Ministry of SMEs and Startups, Republic of Korea (S3045542); the Technology Innovation Program (20003747, Development of high-performance cathode material manufacturing technology through valuable metal upcycling from waste batteries and waste cathode material) funded by the Ministry of Trade, Industry & Energy (MOTIE, Korea); and the Korea Agency for Infrastructure Technology; the National Research Foundation of Korea(NRF) funded by the Korea government (MSIT) (No.2021R1F1A1063481) and Korea Institute for Advancement of Technology(KIAT) grant funded by the Korea Government(MOTIE)(P0020614, HRD Program for Industrial Innovation).

REFERENCES

[1] W. Liu, P. Oh, X. Liu, M. J. Lee, W. R. Cho, S. J. Chae, Y. S. Kim and J. Cho, *Angew Chem Int Ed.,* 54 (15), 4440-4457 (2015)
[2] Y. Xia, J. Zheng, C. Wang and M. Gu, *Nano Energy*., 49, 434-452 (2018)
[3] W. Zhao, L. Zou, J. Zheng, H. Jia, J. Song, M. H. Engelhard, C. Wang, W. Xu, Y. Yang and J. Zhang, Adv Energy Mater., 11 (13), 2211-2220 (2018)
[4] X. Li, K. Zhang, D. Mitlin, Z. Yang, M. Wang, Y. Tang, F. Jiang, Y. Du and J. Zheng, Chem Mater. 30 (8), 2566-2573 (2018)
[5] D. W. Wang, R. H. Kou, Y. Yang, C. J. Sun, H. Zhao, M. J. Zhang, Y. Li, H.A. Huq, J. Y. P. Ko, F. Pan, Y. K. Sun, Y. Yang, K. Amine, J. Bai, Z. H. Chen and F. Wang, Adv Mater. 29, 160675 (2017).
[6] J. B. Goodenough and Y. S. Kim, Chem Mater. 22 (3), 587-603 (2010)
[7] C. Liu, F. Li, LP. Ma and H. M. Cheng, Adv Mater. 22 (8), E28-E62 (2010)
[8] N. Yabuuchi and T. Ohzuku, J Power Sources. 119 (21), 171-174 (2003)
[9] C. Li, H.P. Zhang, L. J. Fu, H. Liu, Y.P. Wu, E. Rahm, R. Holze and H.Q. Wu, Electrochim Acta. 51 (19), 3872-3883 (2006)
[10] Y. Kim, H. S. Kim and S. W. Martin, Electrochim Acta. 52 (3), 1316-1322 (2006)
[11] N. Yabuuchi, K. Yoshii, S. T. Myung, I. Nakai and S. Komaba, J Am Chem Soc. 133 (12), 4404-4419 (2011)
[12] J. H. Jo, C. H. Jo, H. Yashiro, S. J. Kim and S. T. Myung, J Power Sources. 313, 1-8 (2016)
[13] X. Xiong, Z. Wang, P. Yue, H. Guo, F. Wu, J. Wang and X. Li, J Power Sources. 222, 318-325 (2013)
[14] K. Tasaki, A. Goldberg, J. J. Lian, M. Walker, A. Timmons and S. J. Harris, J Electrochem Soc. 156 (12), 1019 (2009)
[15] Y. Bi, T. Wang, M. Liu, R. Du, W. Yang, Z. Liu, Z. Peng, Y. Liu, D. Wang and X. Sun, RSC Adv. 6 (23), 19233-19237 (2016)

[16] J. H. Park, B. J. Choi, Y. S. Kang, S. Y. Park, D. J. Yun, I. S. Park, J. H. Shim, J. H. Park, H. N. Han and K. J. Park, Energy Technol. 6 (7), 1361-1369 (2018)
[17] K. Park, J. H. Park, S. G. Hong, B. Choi, S. Heo, S. W. Seo, K. M. Min and J. H. Park, Sci Rep. 7 (1), 44557 (2017)
[18] J. K. Yang, Y. H. Jin, D. H. Yang and D. W. Kim, J Korean Cryst Growth Cryst Technol. 29 (5), 222-228 (2019)
[19] J. Ge, L. Zhang, J. Lu, J. Zhu and S. Jiao, J Electrochem Soc. 163 (10), 300-304 (2016)
[20] Swonger L. Producing lithium. U.S Patent Application US2015/0014184A. Vol. 1; 2015.
[21] L. Cai, Z. Liu, K. An and C. Liang, J Electrochem Soc. 159 (7), 924-928 (2012)
[22] R. Stoyanova, E. Zhecheva, E. Kuzmanova, R. Alcántara, P. Lavela and J. L. Tirado, Solid State Ionics. 128 (1-4), 1-10 (2000)

NOMENCLATURE

°C	temperature
g	weight
V	Voltage

Greek symbols

λ	wavelength
θ	angle
μ	Micro- (one millionth)